

1 **The application of land use regression model to investigate spatiotemporal variations**  
2 **of PM<sub>2.5</sub> in Guangzhou, China: Implications for the public health benefits of PM<sub>2.5</sub>**  
3 **reduction**

4 Yangzhi Mo <sup>a, b, c</sup>, Douglas Booker <sup>c, d</sup>, Shizhen Zhao <sup>a, b</sup>, Jiao Tang <sup>a, b</sup>, Hongxing Jiang <sup>a, b</sup>,  
5 Jin Shen <sup>e</sup>, Duohong Chen <sup>e</sup>, Jun Li <sup>a, b</sup>, Kevin C Jones <sup>d</sup>, Gan Zhang <sup>a, b\*</sup>

6

7 <sup>a</sup> State Key Laboratory of Organic Geochemistry and Guangdong-Hong Kong-  
8 Macao Joint Laboratory for Environmental Pollution and Control, Guangzhou Institute of  
9 Geochemistry, Chinese Academy of Sciences, Guangzhou, 510640, China

10 <sup>b</sup> CAS Center for Excellence in Deep Earth Science, Guangzhou, 510640, China

11 <sup>c</sup> National Air Quality Testing Services, Lancaster Environment Centre, Lancaster  
12 University, Lancaster LA1 4YQ, United Kingdom

13 <sup>d</sup> Lancaster Environment Centre, Lancaster University, Lancaster LA1 4YQ, United  
14 Kingdom

15 <sup>e</sup> Guangdong Environmental Protection Key Laboratory of Secondary Air Pollution  
16 Research, Guangdong Environmental Monitoring Center, Guangzhou, China

17

18 \* Corresponding author: Dr. Gan Zhang

19 Tel: +86-20-85290805; Fax: +86-20-85290706; E-mail: zhanggan@gig.ac.cn

20

21

22

23

## 24 **Abstract**

25       Understanding the intra-city variation of PM<sub>2.5</sub> is important for air quality management  
26 and exposure assessment. In this study, to investigate the spatiotemporal variation of PM<sub>2.5</sub>  
27 in Guangzhou, we developed land use regression (LUR) models using data from 49 routine  
28 air quality monitoring stations. The R<sup>2</sup>, adjust R<sup>2</sup> and 10-fold cross validation R<sup>2</sup> for the  
29 annual PM<sub>2.5</sub> LUR model were 0.78, 0.72 and 0.66, respectively, indicating the robustness  
30 of the model. In all the LUR models, traffic variables (e.g., length of main road and the  
31 distance to nearest ancillary) were the most common variables in the LUR models,  
32 suggesting vehicle emission was the most important contributor to PM<sub>2.5</sub> and controlling  
33 vehicle emissions would be an effective way to reduce PM<sub>2.5</sub>. The predicted PM<sub>2.5</sub> exhibited  
34 significant variations with different land uses, with the highest value for impervious surfaces,  
35 followed by green land, cropland, forest and water areas. Guangzhou as the third largest city  
36 that PM<sub>2.5</sub> concentration has achieved CAAQS Grade II guideline in China, it represents a  
37 useful case study city to examine the health and economic benefits of further reduction of  
38 PM<sub>2.5</sub> to the lower concentration ranges. So, the health and economic benefits of reducing  
39 PM<sub>2.5</sub> in Guangzhou was further estimated using the BenMAP model, based on the annual  
40 PM<sub>2.5</sub> concentration predicted by the LUR model. The results showed that the avoided all  
41 cause mortalities were 992 cases (95% CI: 221–2140) and the corresponding economic  
42 benefits were 1478 million CNY (95% CI: 257–2524) (willingness to pay approach) if the  
43 annual PM<sub>2.5</sub> concentration can be reduced to the annual CAAQS Grade I guideline value  
44 of 15 µg/m<sup>3</sup>. Our results are expected to provide valuable information for further air  
45 pollution control strategies in China.

46 **Keywords:** PM<sub>2.5</sub>, Land use regression model, BenMAP, Guangzhou, Health benefit

## 47 **1. Introduction**

48 Ambient particle matter (PM) has been recognized as a great threat to human health  
49 and has received worldwide attention. Numerous epidemiological studies have shown that  
50 long-term exposure to fine particulate matter (PM<sub>2.5</sub>, particles with aerodynamic diameter  
51 smaller than 2.5µm) is associated with many adverse health effects, such as respiratory and  
52 cardiovascular diseases, and an increase of mortality (Beelen et al., 2014; Chen et al., 2018b;  
53 Chen et al., 2012; Stafoggia et al., 2014). In addition, PM<sub>2.5</sub> is also responsible for climate  
54 deterioration and haze episodes that exert negative impacts on the living environment  
55 (Huang et al., 2014; Wu et al., 2005). Moreover, more than half of the global population live  
56 in high-density urban environments where these adverse effects are expected to be stronger  
57 (Jin et al., 2019; Yuan et al., 2014). However, intra-city variations of PM<sub>2.5</sub> have been shown  
58 to be significant, thus, it is critical for air quality management and exposure risk assessment  
59 to accurately estimate the spatial distribution of PM<sub>2.5</sub> within cities.

60  
61 Early studies mostly used data from fixed monitoring stations to present regional PM<sub>2.5</sub>  
62 concentrations, but it is generally difficult to capture intra-city variability due to the limited  
63 geographic coverage of monitoring stations (West et al., 2016). To address such challenges,  
64 previous studies tried to combine monitoring data and spatial interpolation (e.g. kriging and  
65 inverse distance weighted interpolation)(Meng et al., 2015). However, interpolation  
66 methods are considered too mechanistic and can produce overly smoothed concentration  
67 surfaces, and cannot consider environmental characteristics (Meng et al., 2015; Zou et al.,  
68 2015). Alternatively, air quality models (e.g., chemical transport models and dispersion  
69 models) could estimate spatiotemporal variations of air pollution concentrations,

70 considering the emission sources, meteorology and topography conditions. However, the  
71 simulated results of air quality models are highly reliant on the accuracies of emission  
72 inventories, which usually makes the simulation process complicated and high-cost (de  
73 Hoogh et al., 2014; Solomos et al., 2015; Zhang et al., 2012). Satellite-based aerosol optical  
74 depth (AOD) data has also popularly applied to predict ground-level PM<sub>2.5</sub>, but this method  
75 is limited by the imaging time and the spatial resolution is relatively coarse (Ma et al., 2016;  
76 Zang et al., 2017). In addition, the relationship between PM<sub>2.5</sub> and AOD could be affected  
77 by PM optical properties, PM vertical and diurnal concentration profiles, and meteorological  
78 conditions (Lee et al., 2011). Compared with the above methods, the land use regression  
79 (LUR) model was shown to be able to capture intra-city variations of air pollutants at a  
80 refined spatial scale with a relatively low demand for data input (Briggs et al., 1997; Hoek  
81 et al., 2008). In LUR models, the concentration of air pollutants at unmonitored sites could  
82 be predicted by a linear regression framework based on spatial predictors that include  
83 emission sources (e.g. land use, traffic, population density and nearby pollutant emissions)  
84 and dispersion conditions (e.g. elevation, boundary layer height, meteorology) (Chen et al.,  
85 2018b; Meng et al., 2015; Sampson et al., 2013; Wu et al., 2005; Young et al., 2016).  
86 Especially, the real time meteorological parameters (e.g., temperature, wind speed and  
87 relative humidity) and anthropogenic activities related pollutants (e.g., NO<sub>2</sub> and CO) can be  
88 combined into the linear regression frameworks to develop high time resolution grid-scale  
89 models (Hsieh et al., 2020; Lee et al., 2016). With the development of Geographic  
90 Information System (GIS) technology, LUR models have been shown to be a cost-effective  
91 approach to estimate spatial variations of air pollutants in different regions of the world  
92 (Briggs et al., 1997; Chen et al., 2018b; Hoek et al., 2008; Meng et al., 2015; Vienneau et

93 al., 2013; Zou et al., 2015). Also, in recent years LUR models have been widely used to  
94 assess air pollutants exposures in epidemiological research (Beelen et al., 2014; Chen et al.,  
95 2017b).

96

97 Evaluating the health impacts and benefits associated with air quality improvements is  
98 essential for governments and policy makers. In recent years, the Environmental Benefits  
99 Mapping and Analysis Program Community Edition (BenMAP-CE) developed by the  
100 United States Environmental Protection Agency (USEPA) has been widely used to estimate  
101 health benefits of PM<sub>2.5</sub> reduction at local, regional, and national scales (Chen et al., 2017b;  
102 Kheirbek et al., 2014; Li et al., 2019; Sacks et al., 2018). The reliability of BenMAP  
103 estimates highly depend on the accuracy and suitability of air quality exposure fields used  
104 in benefit calculations. However, it should be noted that the exposure PM<sub>2.5</sub> fields in  
105 previous studies that used BenMAP were mostly generated by chemical transport models  
106 and interpolation methods (Chen et al., 2017b; Luo et al., 2020). Given the advantages of  
107 using a LUR model that were mentioned above, the combination of a LUR model and  
108 BenMAP could help better estimate health benefits associated with PM<sub>2.5</sub> reduction.

109

110 To reduce the PM<sub>2.5</sub> concentration and minimize its adverse influence on human health,  
111 the China State Council released a 5-year Air Pollution Prevention and Control Action Plan  
112 in 2013. From 2013 to 2017, the nationwide-average annual PM<sub>2.5</sub> concentrations decreased  
113 from 67.8 µg/m<sup>3</sup> to 45.6 µg/m<sup>3</sup> (Wu et al., 2020). These concentration reductions were seen  
114 especially in the Pearl River Delta (PRD) region where in 2017 the annual PM<sub>2.5</sub>  
115 concentration already met the Chinese Ambient Air Quality Standards (CAAQS, GB3095-

116 2012) Grade II guidelines ( $35 \mu\text{g}/\text{m}^3$ ) (Shen et al., 2020). In Guangzhou, the main city of the  
117 PRD region annual  $\text{PM}_{2.5}$  concentrations in the past three years (2017 to 2019) were lower  
118 than  $35 \mu\text{g}/\text{m}^3$ , due to emission control measures and favorable meteorological conditions.  
119 However, there is still a distance to reach the annual Grade I guideline of  $15 \mu\text{g}/\text{m}^3$  proposed  
120 by CAAQS. In addition, the  $\text{PM}_{2.5}$  concentrations of Guangzhou were higher in fall and  
121 winter due to the unfavorable meteorological conditions for pollutant dispersion. Therefore,  
122 there remains a need to better understand the spatial and temporal variation of  $\text{PM}_{2.5}$  in  
123 Guangzhou. Moreover, as Chinese air quality has improved a lot in recent years, the  $\text{PM}_{2.5}$   
124 concentrations in many cities have fallen below Grade II guideline ( $35 \mu\text{g}/\text{m}^3$ ). Guangzhou  
125 as the third biggest city in China with relatively lower  $\text{PM}_{2.5}$ , it represents a useful case study  
126 city to examine the health and economic benefits of further reduction of  $\text{PM}_{2.5}$  to the lower  
127 concentration ranges. This could provide valuable information for future efforts to reduce  
128 air pollution in China.

129  
130 The purpose of this study was therefore to: (1) develop seasonal and annual LUR  
131 models based on 49 routine air quality monitoring stations, to investigate the spatiotemporal  
132 variation of  $\text{PM}_{2.5}$  in Guangzhou; (2) estimate public health benefits of reducing  $\text{PM}_{2.5}$  to  
133 CAAQS Grade I guidelines ( $15 \mu\text{g}/\text{m}^3$ ) by combining LUR modelling and BenMAP. Our  
134 results are expected to help policymakers to improve air quality and achieve health and  
135 economic benefits for citizens.

## 137 **2. Methodology**

### 138 **2.1 Study area**

139 Guangzhou (22°26'–23°56'N, 112°57'–114°3'E, Figure 1) is the capital and most  
140 populous city of the province of Guangdong in Southern China. On the Pearl River about  
141 120 km north-northwest of Hong Kong and 145 km north of Macau, Guangzhou serves as  
142 a major port and transportation hub. Guangzhou is China's third largest city with a  
143 population of 14.9 million in 2018, covering an area of 7,434 km<sup>2</sup> with a typical subtropical  
144 monsoon climate.

## 145

### 146 **2.2 Ground PM<sub>2.5</sub> monitoring data**

147 The daily PM<sub>2.5</sub> concentration data of 2018 were obtained from the air pollution  
148 monitoring network operated by the Guangdong Environmental Monitoring Centre. There  
149 are 49 routine monitoring stations included in this study (Figure 1). The daily concentrations  
150 were only included in calculations when there were at least 18 hours of valid data per day.  
151 The PM<sub>2.5</sub> measurement and quality control follow the regulation of the CAAQS (No.  
152 GB3095-2012). To investigate the spatiotemporal variation of PM<sub>2.5</sub> in Guangzhou, the  
153 seasonal average PM<sub>2.5</sub> concentrations were calculated and served as dependent variables of  
154 seasonal LUR models.

### 155

### 156 **2.3 Geographical data**

157 As presented in Table 1, we employed a combination of point, buffer, and proximity  
158 based geographic variables. A total of 352 predictor variables were considered. Each  
159 predictor variable was first given an expected direction of the regression coefficient (e.g.,  
160 positive or negative). We used the ESRI ArcGIS 10.5 to extract predictor variables from  
161 GIS layers.

162

163 We obtained the road data from OpenStreetMap (<https://www.openstreetmap.org>).  
164 Considering the jurisdiction and function, we divided the roads into four categories: main  
165 roads (freeways, such as motorways and trunk ways, usually with limited access), highways  
166 (primary roads, important roads that often link towns or main road within cities), ancillary  
167 (tertiary roads, such as residential roads, which serve as an access to housing or within a  
168 community), and alley (residential roads, pedestrian walkways, and tracks). It should be  
169 noted that, because it is difficult to obtain the traffic intensity, we used the distance to nearest  
170 road and length of road to represent traffic related variables. Compared to traffic intensity  
171 which could indicate the number of vehicles, the road information in GIS just represented  
172 as one-dimensional lines that cannot reflect the number of vehicles, width of road, and the  
173 number of lanes. However, previous studies have found that the performance of LUR models  
174 developed with lengths of road were comparable to those using traffic intensity data for  
175 explaining the refined spatial variability of pollutant concentrations (Henderson et al., 2007;  
176 Rosenlund et al., 2007). Therefore, we considered distance to nearest road and road length  
177 as appropriate traffic related variables, in the absence of traffic intensity.

178

179 Land use data were derived from International Symposium on Land Cover Mapping  
180 (<http://data.ess.tsinghua.edu.cn/>), with a resolution of 30 m. The land use types were  
181 classified into bare land, cropland, forest, grassland, impervious surfaces, shrubland, water  
182 bodies, and wetland. The impervious surfaces were further separated into residential area,  
183 commercial area, industrial area, transportation area, public management and service area.  
184 The nearest distance to the coast of each monitoring site was also calculated based on the

185 coastline shapefile of China.

186  
187 The population density data with approximately 1 km resolution in 2015 were obtained  
188 from the Landsat global population database, which was developed by the United States  
189 Department of Energy's Oak Ridge National Laboratory (<https://www.worldpop.org/>).  
190 Meanwhile, the gridded GDP data were provided by Resources and Environment Data  
191 Cloud Platform (<http://www.resdc.cn>). We downloaded the Digital Elevation Model (DEM)  
192 data from Shuttle Radar Topography Mission (SRTM, <http://srtm.csi.cgiar.org>), and the  
193 spatial resolution was 90 m. The locations of bus stops and parking areas were extracted  
194 using Amap Application Programming Interface (API) based on categories and keywords  
195 (<https://lbs.amap.com/api/uri-api>) The monthly meteorological data (e.g. boundary layer  
196 height, temperature, precipitation, pressure, and wind speed) were extracted from the Third  
197 Pole Environment Database (<http://en.tpedatabase.cn/>).

## 199 **2.4 LUR model development, validation and mapping**

200 The annual and seasonal concentrations of  $PM_{2.5}$  and geographic variables were used  
201 for the LUR model development. We followed the manually supervised forward multiple  
202 linear regression method to develop the LUR models for  $PM_{2.5}$  (Eeftens et al., 2012a).  
203 Briefly, the  $PM_{2.5}$  concentrations were considered as dependent variables, while the  
204 geographic variables were used as independent variables. The model construction started by  
205 including predictor variables with the highest adjusted  $R^2$  in univariate regressions analysis.  
206 Thereafter, the candidate variables were added into the model if they satisfied the following  
207 criteria; (1) the adjusted  $R^2$  of the model increased by at least 1%; (2) the  $p$  value of the

208 variable was  $< 0.05$ ; (3) the variance inflation factor (VIF, a check for multi-collinearity) of  
209 the variable was  $< 3$ ; (4) the coefficient of the variable accorded with the prior direction and  
210 variables already in the model did not change their regression directions. All possible  
211 predictor variables were added until no predictor variables added more than 1% to the  
212 adjusted  $R^2$  of the previous regression model.

213  
214 We used the 10-fold cross-validation method to evaluate overall model performance.  
215 The adjusted  $R^2$  and root mean squared error (RMSE) between the predicted and measured  
216 concentrations for all sites were calculated to present the model's fit. In addition, Moran's I  
217 was calculated to evaluate the spatial autocorrelation of the residuals. All the statistical  
218 analyses were conducted by R software (Version 3.2.2).

219  
220 The predicted  $PM_{2.5}$  concentration surfaces were created according to the final LUR  
221 models. The study area was divided into 7,225  $1000 \times 1000$  m grid cells. The predictor  
222 variables of LUR model were drawn around the centroids of each grid cell and the  $PM_{2.5}$   
223 concentrations were calculated by the final LUR model coefficients. At last, we applied  
224 universal kriging interpolation to draw  $PM_{2.5}$  concentrations map across Guangzhou. It  
225 should be noted that the reliability of predicted  $PM_{2.5}$  concentrations maybe lower in areas  
226 with sparse monitoring stations, especially for the Northeast of Guangzhou (Figure 1).

## 227 228 **2.5 Health impacts and economic benefits estimates**

229 In this work, BenMAP-CE 1.5 was used to estimate the health and economic benefits  
230 of  $PM_{2.5}$  reductions. Since previous studies showed that more than 90% of health impacts

231 of PM<sub>2.5</sub> were from mortality, we selected avoidable premature mortality to present the  
232 health benefits of PM<sub>2.5</sub> reductions (DeMocker, 2003). According to the International  
233 Classification of Diseases Revision 10 (ICD-10), the causes of death in this study are  
234 classified into all causes (A00–R99), cardiovascular diseases (I00–I99), and respiratory  
235 diseases (J00–J98). The health impacts are estimated by BenMAP-CE according to  
236 following the equation (Davidson et al., 2007):

237

$$238 \quad \Delta Y = Y_0(1 - e^{-\beta\Delta PM}) * Pop \quad (1)$$

$$239 \quad \beta_{\min} = \beta - (1.96 \times \sigma_{\beta}) \quad (2)$$

$$240 \quad \beta_{\max} = \beta + (1.96 \times \sigma_{\beta}) \quad (3)$$

241

242 where  $\Delta Y$  is the avoided premature mortalities due to the PM<sub>2.5</sub> reductions,  $Y_0$  is the  
243 baseline incidence rate for the health endpoint (mortality),  $\Delta PM$  ( $\mu\text{g}/\text{m}^3$ ) is the annual PM<sub>2.5</sub>  
244 concentration change, Pop (person) is the exposed population,  $\beta$  is the exposure  
245 concentration-response coefficient, representing the percent change in a certain health  
246 impact per unit of PM<sub>2.5</sub> concentration, and  $\sigma_{\beta}$  is the standard error of  $\beta$  (Table S1).

247

248 For this work, Guangzhou was divided into 7,225 1000×1000 m grids. The PM<sub>2.5</sub>  
249 annual mean concentration in each grid was estimated based on the LUR model. The control  
250 case concentration was rolled back to annual Grade I guidelines of 15  $\mu\text{g}/\text{m}^3$  proposed by  
251 CAAQS. The gridded population data in 2018 with 1 km<sup>2</sup> resolution was calculated by  
252 multiplying the each 1 km<sup>2</sup> grid in 2015 by the Guangzhou population ratio of 2018/2015.  
253 The baseline incidence data for all-cause, cardiovascular diseases, and respiratory diseases

254 in 2018 were obtained from the Guangdong Statistical Yearbook  
255 (<http://stats.gd.gov.cn/gdtjnj/>).

256  
257 BenMAP-CE uses a Monte Carlo approach (5000 times) and specifies Latin hypercube  
258 points to generate 95% confidence intervals around mean prediction of  $\beta$  values of each  
259 health endpoint. Then the BenMAP-CE estimates the incidence of changes in each grid  
260 according to the assumption value of  $\beta$  and generates the distribution of the incidence  
261 changes.

262  
263 We further evaluated the economic benefits of the health impacts associated with the  
264  $PM_{2.5}$  reduction. The willingness to pay (WTP), cost of illness (COI), and human capital  
265 (HC) methods are commonly used to quantify the economic benefits associated with  
266 avoided mortality. Generally, WTP is the most widely preferred used method, because it  
267 takes intangible losses into account, such as pain, suffering and other adverse effects due to  
268 illness (Robinson, 2011). Thus, the WTP method was used to evaluate the economic benefits  
269 from avoided premature mortality, and the unit economic values associated with premature  
270 mortality were summarized in Table S2. We converted the US dollar to Chinese Yuan (CNY)  
271 based on Purchasing Power Parity adjusted exchange rates, and the unit value for various  
272 currency years was adjusted to the year 2018 by multiplying by the annual consumer price  
273 index (CPI) in China.

### 274 275 **3. Results and discussion**

#### 276 **3.1 Descriptive statistics for $PM_{2.5}$ concentrations**

277 The monitored annual average concentration of PM<sub>2.5</sub> was  $34.4 \pm 21.0 \mu\text{g}/\text{m}^3$ , which  
278 was lower than annual CAAQS Grade II guidelines ( $35 \mu\text{g}/\text{m}^3$ ). However, it should be noted  
279 that, the concentration of PM<sub>2.5</sub> exhibited significant seasonal variation (Figure 2), which  
280 showed highest concentrations in winter ( $46.7 \pm 31.0 \mu\text{g}/\text{m}^3$ ), followed by the fall ( $37.0 \pm$   
281  $14.0 \mu\text{g}/\text{m}^3$ ), spring ( $35.6 \pm 16.8 \mu\text{g}/\text{m}^3$ ), and summer ( $22.6 \pm 8.0 \mu\text{g}/\text{m}^3$ ). The higher  
282 concentrations of PM<sub>2.5</sub> in winter are associated with the unfavorable meteorological  
283 conditions (e.g. lower wind speed, precipitation, and boundary layer height) for pollutants  
284 dispersion (Chen et al., 2018a; Chen et al., 2018c). In addition, the emissions of PM<sub>2.5</sub> would  
285 also increase due to cold start-up of automobiles in the lower winter temperatures (Zhang et  
286 al., 2015b). In fact, there were 52 days (57.8%) and 14 days (15.7%) of daily PM<sub>2.5</sub>  
287 concentrations in winter above current daily CAAQS Grade I ( $35 \mu\text{g}/\text{m}^3$ ) and II ( $75 \mu\text{g}/\text{m}^3$ )  
288 guidelines, followed by fall (48.9% and 1.1%), spring (38.9% and 4.4%), and summer (10%  
289 and 0%). It is therefore important to investigate spatiotemporal variation of PM<sub>2.5</sub> and further  
290 strengthen efforts to control the atmospheric pollutants in Guangzhou.

### 292 3.2 PM<sub>2.5</sub> LUR models and evaluation

293 The annual and seasonal LUR models for PM<sub>2.5</sub> in Guangzhou are shown in Table 2.  
294 There were 4 to 5 predictive variables in the final LUR models. The VIF values of all the  
295 variables were  $< 3$ , indicating a relatively low multicollinearity between the predictive  
296 variables. The Moran's I value of the models ranged from 0.01 to 0.12 with  $p$  values lower  
297 than 0.05, which indicated no significant spatial autocorrelation of the residuals.

298  
299 For the annual PM<sub>2.5</sub> models, five predictive variables remained in the final LUR model,

300 including the length of main roads (4000m buffer), DEM, distance to nearest ancillary,  
301 commercial area (1000m buffer), and wind speed. The predicted annual average PM<sub>2.5</sub>  
302 concentrations are mapped in Figure 3. The predicted annual PM<sub>2.5</sub> concentrations were 35.5  
303 ± 9.29 µg/m<sup>3</sup>, which are close to the measured values across 49 monitoring stations. As  
304 expected, the PM<sub>2.5</sub> concentrations increased with the length of main road and commercial  
305 area, while DEM, distance to nearest ancillary and wind speed were negatively correlated  
306 with PM<sub>2.5</sub> concentrations. Thus, we found that the higher PM<sub>2.5</sub> concentrations occurred in  
307 the center of Guangzhou with a relatively intensive road network and commercial area,  
308 whereas lower concentrations areas distributed in the north and south Guangzhou suburbs  
309 with fewer roads (Figure 3).

310

311 For the seasonal models, we found that the predicted seasonal and annual PM<sub>2.5</sub>  
312 concentrations across 7,225 1000×1000 m grids exhibited a good correlation with each other  
313 (Table S3). This indicated that the PM<sub>2.5</sub> concentrations might be affected by similar factors  
314 throughout the year. Indeed, the predictive variables of seasonal models were similar to  
315 those in the annual model. In addition, the predictive variables left in the models could also  
316 be used to identify potential sources of air pollutants. In this work, we found that all the  
317 models contained traffic related variables (e.g. distance to nearest ancillary and length of  
318 main road), suggesting that vehicle emissions were an important contributor to PM<sub>2.5</sub> and  
319 controlling vehicle emissions would be an effective way to reduce PM<sub>2.5</sub> in Guangzhou. That  
320 is consistent with previous studies which reported that 20 to 47% of PM<sub>2.5</sub> in Guangzhou  
321 derived from mobile sources (Liu et al., 2014; Yuan et al., 2018). The distance to nearest  
322 ancillary entered all the LUR models and was a strong predictor variable. That may be

323 because the speed of vehicles on ancillary roads is usually limited to below 40 km/h in China,  
324 and the emissions of  $PM_{2.5}$  and gaseous precursors of  $PM_{2.5}$  from vehicles tend to be higher  
325 at lower speeds (Jones and Harrison, 2006; Wang et al., 2013). Another important traffic  
326 related variable is the length of main road. Although the speed of vehicles on main roads is  
327 relatively high, traffic on main roads is much higher. Therefore, the length of main roads  
328 was treated as a predictive variable in 3/5 of LUR models.

329  
330 Meteorology has been shown to play a significant role in the distribution of air  
331 pollution (Chen et al., 2018a; Chen et al., 2018c). However, most previous studies did not  
332 incorporate meteorological variables in LUR models in China. In this work, all the LUR  
333 models contained the meteorological variables (e.g. wind speed and precipitation). We found  
334 that the  $PM_{2.5}$  concentration decreased with the increasing wind speed and precipitation. In  
335 fact, the wind would facilitate dispersion of  $PM_{2.5}$ , while the rain would clean ambient  $PM_{2.5}$   
336 through the wash-out effect.

337  
338 In this study, only three buffer predictive variables with buffer sizes  $< 700$  m enter the  
339 final LUR model (Table 2), while most of buffer predictive variables (7/10) in the final LUR  
340 models have a larger buffer buffers size ( $> 1000$  m). Therefore, the final LUR models might  
341 be sensitive to variables with larger buffers. In general,  $PM_{2.5}$  could be directly emitted from  
342 primary sources, and secondarily formed from precursors by various atmospheric chemical  
343 reactions (Lai et al., 2016; Liu et al., 2014; Wang et al., 2018; Yuan et al., 2018). Moreover,  
344 primary pollutants (e.g., black carbon and heavy metals) tend to be more linked with  
345 variables with smaller buffers, whereas secondary pollutants (e.g.,  $O_3$  and  $NO_3^-$ ) are more

346 associated with variables with larger buffers (Cai et al., 2020; Wu et al., 2015; Zhang et al.,  
347 2015a). Thus, the larger buffer size of variables for PM<sub>2.5</sub> models may suggest the significant  
348 contribution from secondary sources in Guangzhou. Additionally, the larger buffer may  
349 reflect the long-range transport of PM<sub>2.5</sub> from emission sources.

350

351 The LUR models have been widely applied to describe spatial variability in air  
352 pollution concentrations worldwide (Beelen et al., 2013; Chen et al., 2018b; Eeftens et al.,  
353 2012b; Eeftens et al., 2012c; He et al., 2018; Meng et al., 2015; Wu et al., 2015). The  
354 percentage of explained spatial variability ranged from 51% to 88% in the PM LUR models  
355 in Chinese cities (Table 3), which was associated with quality of predictive variables and  
356 measured data, the model development approaches, and the complexity of the study areas.  
357 Our PM<sub>2.5</sub> models' performance was comparable to previous studies in China, which has an  
358 R<sup>2</sup> of 0.62 to 0.82, adjusted R<sup>2</sup> of 0.56 to 0.80, and 10-fold cross-validation (CV) R<sup>2</sup> of 0.50  
359 to 0.78 (Table 3). The model R<sup>2</sup> values were close to those of CV R<sup>2</sup>, suggesting the good  
360 robustness of our LUR models. Moreover, the CV RMSE ranged from 2.29 to 3.00 µg/m<sup>3</sup>,  
361 indicating the predicted values coincided well with the measured values. We found that the  
362 performance of the models exhibited significant seasonal variation, which showed highest  
363 explained spatial variability in winter (80%), followed by fall (62%), spring (60%) and  
364 summer (56%). This may be due to the fact that it is difficult for the LUR model to predict  
365 PM<sub>2.5</sub> formed from secondary sources, and the contribution of secondary sources to PM<sub>2.5</sub>  
366 would be higher in warm seasons.

367

368 As shown in Table 3, most PM LUR models in China were developed by the routine

369 monitoring stations data from government (Chen et al., 2018b; He et al., 2018; Meng et al.,  
370 2015; Wu et al., 2015). However, the number of routine monitoring stations is limited in  
371 most Chinese cities, which cannot meet the minimum required number of sampling sites  
372 suggested for LUR model development (40 to 80 sites) (Hoek et al., 2008). In addition,  
373 routine monitoring stations were generally designed for regulatory purposes, with few sites  
374 situated close to traffic or industrial sources. To overcome such challenges, some studies  
375 have used purposefully designed monitoring networks to build their LUR models (Cai et al.,  
376 2020; Eeftens et al., 2012c; Jin et al., 2019; Zhang et al., 2015a). Although the purpose-  
377 designed monitoring sites have sufficient geographic coverage to capture the gradients of  
378 spatial predictive variables, it should be noted that purpose-designed monitoring campaigns  
379 can be money- and time-consuming (Beelen et al., 2013; Briggs et al., 1997; Eeftens et al.,  
380 2012a). Additionally, the sampling period for purpose-designed monitoring campaigns is  
381 usually within several weeks, which can introduce uncertainties in the models.

382

383 In this study, the number of routine monitoring stations (49 stations) was more than  
384 previous LUR models for Chinese cities based on routine monitoring stations data, and  
385 comparable to other studies with purpose-designed monitoring data. In addition, we  
386 obtained the PM<sub>2.5</sub> data from routine monitoring stations is a relatively cost-effective  
387 procedure without additional sampling, and the measurements were continuous in temporal  
388 coverage. Moreover, most of the routine monitoring stations in Guangzhou were located in  
389 the urban centre with high population density, suggesting the data and the LUR models are  
390 suitable for PM<sub>2.5</sub> human exposure assessment.

391

### 3.3 Seasonal and spatial variation of predicted PM<sub>2.5</sub>

The seasonal pattern of predicted average PM<sub>2.5</sub> concentrations was consistent with that of measured values, which exhibited highest values in winter ( $43.8 \pm 9.6 \mu\text{g}/\text{m}^3$ ), followed by fall ( $35.6 \pm 7.2 \mu\text{g}/\text{m}^3$ ), spring ( $35.3 \pm 12.7 \mu\text{g}/\text{m}^3$ ), and summer ( $20.7 \pm 5.8 \mu\text{g}/\text{m}^3$ ). In addition, the intercept of LUR models showed similar variation patterns to the predicted values (Table 2), which is higher in winter and fall. This suggested that the intercept of LUR models could be employed to reflect the seasonal variations (Chen et al., 2017c; Sabaliauskas et al., 2015; Wu et al., 2015).

The spatial variations of PM<sub>2.5</sub> were similar across seasons. The PM<sub>2.5</sub> was higher in the center of Guangzhou where there is a more intensive road network, and a larger commercial area (Figure 4). The north and south of Guangzhou had lower PM<sub>2.5</sub> concentrations, which may be due to them being away from the pollutant sources. In addition, the more forested areas in the north may help filter the PM<sub>2.5</sub>, while proximity to the coast in the south may promote dispersion of PM<sub>2.5</sub>.

Previous studies have reported that PM concentrations could be influenced by land use types (Anand and Monks, 2017; Tang et al., 2018), so it is important to investigate the distribution of PM in different land use types. Due to less than 1% of the areas being bare land and wetland we did not take these two land use types into account. In addition, the grassland and shrubland are usually used as roadside and in parks in the cities, so the grassland and shrubland were combined as green land in this study. The contribution of forest, cropland, green land, impervious surface, and water area was 45.3%, 22.7%, 4.5%,

415 21.3% and 6.0%, respectively. Figure 5 shows the predicted PM<sub>2.5</sub> concentration in different  
416 land use types. Regardless of the land use type, we found that all the predicted annual PM<sub>2.5</sub>  
417 concentrations were above the annual CAAQS Grade I guide line, so there is a need to  
418 further reduce the PM<sub>2.5</sub> emissions at source in Guangzhou. In this study, the highest annual  
419 PM<sub>2.5</sub> concentration occurred over impervious surfaces ( $42.3 \pm 6.3 \mu\text{g}/\text{m}^3$ ), followed by  
420 green land ( $38.0 \pm 8.0 \mu\text{g}/\text{m}^3$ ), cropland ( $36.2 \pm 7.4 \mu\text{g}/\text{m}^3$ ), forest ( $33.1 \pm 10.9 \mu\text{g}/\text{m}^3$ ), and  
421 water bodies ( $28.1 \pm 11.0 \mu\text{g}/\text{m}^3$ ). Industrial, commercial and transportation activities and  
422 hence sources are mainly carried out on impervious surfaces, which leads to the highest  
423 PM<sub>2.5</sub> concentrations. The lowest PM<sub>2.5</sub> concentrations were found in water areas, including  
424 rivers and lakes, which is likely related to the water surface removing PM<sub>2.5</sub> via the  
425 absorption effect (Zhu and Zeng, 2018).

426  
427 Vegetation in urban areas (e.g. urban forests, urban parks, and roadside vegetation) is  
428 known to efficiently remove PM (Nowak et al., 2018; Selmi et al., 2016; Wang et al., 2019).  
429 However, the predicted PM<sub>2.5</sub> concentrations varied a lot among the green land, cropland,  
430 and forest. That may be due to the removal efficiency of vegetation being highly dependent  
431 on tree species, leaf surface properties, and seasons (Chen et al., 2017a; Nguyen et al., 2015;  
432 Vos et al., 2013; Wang et al., 2019). The vegetation mainly captures the PM<sub>2.5</sub> via the leaf  
433 surface, and the growth of leaves varies seasonally (Nguyen et al., 2015). However, it should  
434 be noted that Guangzhou has a warm climate, and the vegetation is lush throughout the year.  
435 Thus, it seems the season is not main reason for such differences here. The shrubs and  
436 grasses with lower leaf surface areas and height are the main vegetation species in the green  
437 land, usually found by the roadside and in urban parks close to traffic sources. Thus, the

438 predicted  $PM_{2.5}$  concentration in green land is only second to that in impervious surface. For  
439 the cropland, the combustion of straw residuals may contribute to the relatively high  
440 predicted  $PM_{2.5}$  concentration. Indeed, despite open straw burning being prohibited, biomass  
441 burning is still an important source of  $PM_{2.5}$  in Guangzhou (Lai et al., 2016; Liu et al., 2014).  
442 The forest vegetation in Guangzhou is dominated by tall evergreen trees with large leaf  
443 surface area. These trees are far away from the urban centre area with high pollution. Thus,  
444 the relatively low predicted  $PM_{2.5}$  concentration was observed in the forest area.

### 446 **3.4 Health and economic benefits of $PM_{2.5}$ reduction**

447 The Chinese air quality has greatly improved after the 5-year Air Pollution Prevention  
448 and Control Action Plan that initiated in 2012. Actually, many Chinese cities'  $PM_{2.5}$   
449 concentration achieved CAAQS Grade II guideline at the end of 2017. However, it is  
450 noteworthy that the number of cities'  $PM_{2.5}$  concentration that meet CAAQS Grade I is very  
451 limited. To further improve the air quality in China, it is important to assess the public health  
452 benefits of further reduction of  $PM_{2.5}$  to the lower concentration ranges. Guangzhou as the  
453 third largest city with densely populated in China, of which  $PM_{2.5}$  concentration has  
454 achieved CAAQS Grade II guideline. Therefore, Guangzhou is an ideal case study city to  
455 estimate health and economic benefits of further reduction of  $PM_{2.5}$  to lower concentration  
456 ranges, which can provide valuable information for policy makers to analyze cost and  
457 benefits of air pollution management programs in China. In previous studies, the PM  
458 exposure surfaces imported in the BenMAP were estimated by interpolation methods or  
459 chemical transport models. However, the performance of interpolation methods was affected  
460 by the number and distribution of the monitoring sites, and the stimulation process of

461 chemical transport models was complicated and expensive. Recently, LUR models have  
462 been shown to be an efficient method to assess air pollution exposures in epidemiologic  
463 studies (Chen et al., 2017b; Sampson et al., 2013; Vienneau et al., 2013). Therefore, we  
464 estimated the health and economic benefits of reducing PM<sub>2.5</sub> in Guangzhou using BenMAP  
465 based on the annual PM<sub>2.5</sub> concentration predicted by the LUR model.

466 The estimated values of avoided premature mortality and corresponding economic  
467 benefits are summarized in Table 4. The estimated avoided mortalities from all causes,  
468 cardiovascular, and respiratory were 992 (95% CI: 221–2140), 362 (95% CI: 124–768) and  
469 92 (95% CI: -18–176) cases in 2018 by reducing the annual PM<sub>2.5</sub> concentration to annual  
470 CAAQS Grade I guideline (15 µg/m<sup>3</sup>) respectively. The contribution of cardiovascular and  
471 respiratory to all cause mortalities were 36.5% and 9.3%, respectively. Correspondingly,  
472 economic benefits due to avoided premature mortalities by reducing PM<sub>2.5</sub> were 1478  
473 million CNY (95% CI: 257–2524) based on WTP approach, accounting for 0.064% GDP of  
474 Guangzhou in 2018. Although the BenMAP was widely applied to investigate the public  
475 health benefits of reducing PM<sub>2.5</sub>, there are very limited studies on the estimation of  
476 premature mortalities related to PM<sub>2.5</sub> in Chinese cities. In Shanghai, the avoided all cause  
477 mortalities were estimated to range from 180 to 3500 per year, assuming the PM<sub>2.5</sub>  
478 concentration achieved the annual CAAQS Grade II guideline (35 µg/m<sup>3</sup>), which had an  
479 estimated monetary value ranging from 170 to 1200 million CNY (Voorhees et al., 2014).  
480 For the same scenario, the avoided premature mortalities ranged from 1100 to 4800 per year  
481 in Tianjin, the corresponding economic benefits ranged from 270 to 7200 million CNY  
482 (Chen et al., 2017c). The estimated health and economic benefits of the above two studies  
483 just considered the achievement of meeting the annual CAAQS Grade II guideline. However,

484 due to the annual PM<sub>2.5</sub> concentration in Guangzhou having already achieved the annual  
485 CAAQS Grade II guideline in the past few years, it is difficult to compare the results of  
486 these two studies with Guangzhou. In Guangzhou, the PM<sub>2.5</sub>-related premature mortalities  
487 were estimated to be 1926 cases in 2012, and the reduction of annual PM<sub>2.5</sub> concentration  
488 being greater than 15 µg/m<sup>3</sup> from 2013 to 2015.(Li et al., 2019; Pan et al., 2012). The  
489 estimated avoided mortalities from all causes ranged from 791 to 1473 (Li et al., 2019)  
490 which is comparable to the results of this work. In addition, we only chose mortality as the  
491 health endpoint, while morbidity was not included in this study. Therefore, the health and  
492 economic benefits will be underestimated, and there is a need to further improve the air  
493 quality and public health benefits by reducing PM<sub>2.5</sub> concentration.

494

### 495 **3.5 Limitation and further works**

496 There are several limitations to this study. Source-specific emissions were not  
497 considered in this work, which may be important predictors in the study areas. In addition,  
498 the performance of LUR models in warm seasons was poorer, which may be because the  
499 predictors cannot indicate the secondary formations of PM<sub>2.5</sub> as well. Therefore, to improve  
500 the performances of LUR models, data from air quality models which has considered  
501 emission source inventories and chemical reactions should be incorporated into future LUR  
502 models in Guangzhou (de Hoogh et al., 2016; Yang et al., 2017).

503

504 For the health benefits estimation, we only selected all cause, cardiovascular, and  
505 respiratory mortality as the health endpoints in this work. Moreover, the sex and age of the  
506 population was not considered when estimating the avoided premature mortality. In addition,

507 the LUR models only predict the ambient air pollution concentrations, and the use of  
508 ambient concentration to estimate people's exposure to air pollution may not provide a  
509 reliable result, because more than 80% of people's lives is typically spent indoors (Lim et  
510 al., 2011). All of these may introduce uncertainties into estimation of potential health  
511 benefits of PM<sub>2.5</sub> reduction. Therefore, to enhance the accuracy of health benefits estimation  
512 in future, there is a need to develop the dynamic exposure models that consider differential  
513 exposures between population subgroups (e.g. age and sex) and exposure characteristics in  
514 different microenvironments (Tang et al., 2018).

515

#### 516 **4. Conclusion**

517 In this work, we applied LUR models to study the spatiotemporal variations of PM<sub>2.5</sub>  
518 in Guangzhou. The results showed that all the LUR models had a high accuracy and  
519 predictive ability, and the traffic variables (e.g., length of main roads and the distance to  
520 nearest ancillary) were most common among the LUR models, suggesting that vehicle  
521 emissions were an important source for PM<sub>2.5</sub>. The R<sup>2</sup>, adjusted R<sup>2</sup> and 10-fold cross  
522 validation R<sup>2</sup> of the annual PM<sub>2.5</sub> LUR model were 0.78, 0.72 and 0.66, respectively, which  
523 could provide useful spatial information for air quality management and air pollution  
524 exposure assessment. Therefore, we estimated the health and economic benefits of reducing  
525 PM<sub>2.5</sub> in Guangzhou using BenMAP based on the annual PM<sub>2.5</sub> concentration predicted by  
526 the LUR model. The results showed that, by achieving the annual CAAQS Grade I guideline  
527 (15 µg/m<sup>3</sup>), the avoided all cause mortalities due to exposure to PM<sub>2.5</sub> were 992 cases (95%  
528 CI: 221–2140) and the corresponding economic benefits were 1478 million CNY (95% CI:  
529 257–2524) (willingness to pay approach) in 2018 in Guangzhou.

530

531 **Acknowledgement**

532       The research was funded by the Guangdong Foundation for Program of Science and  
533 Technology Research (2018A050501009, 2017B030314057, 2019A1515011254 and  
534 2019B121205006), Local Innovative Scientific Research Team Project of Guangdong  
535 “Pearl River Talents Plan” (2017BT01Z134), Guangdong provincial science and technology  
536 projects : Guangdong-Hong Kong-Macao Greater Bay Area Urban agglomeration  
537 ecosystem Observation and Research Station (2018B030324002), National Key R&D  
538 Program of China (2017YFC0212000), and Innovate UK and the Newton Fund.

539

540

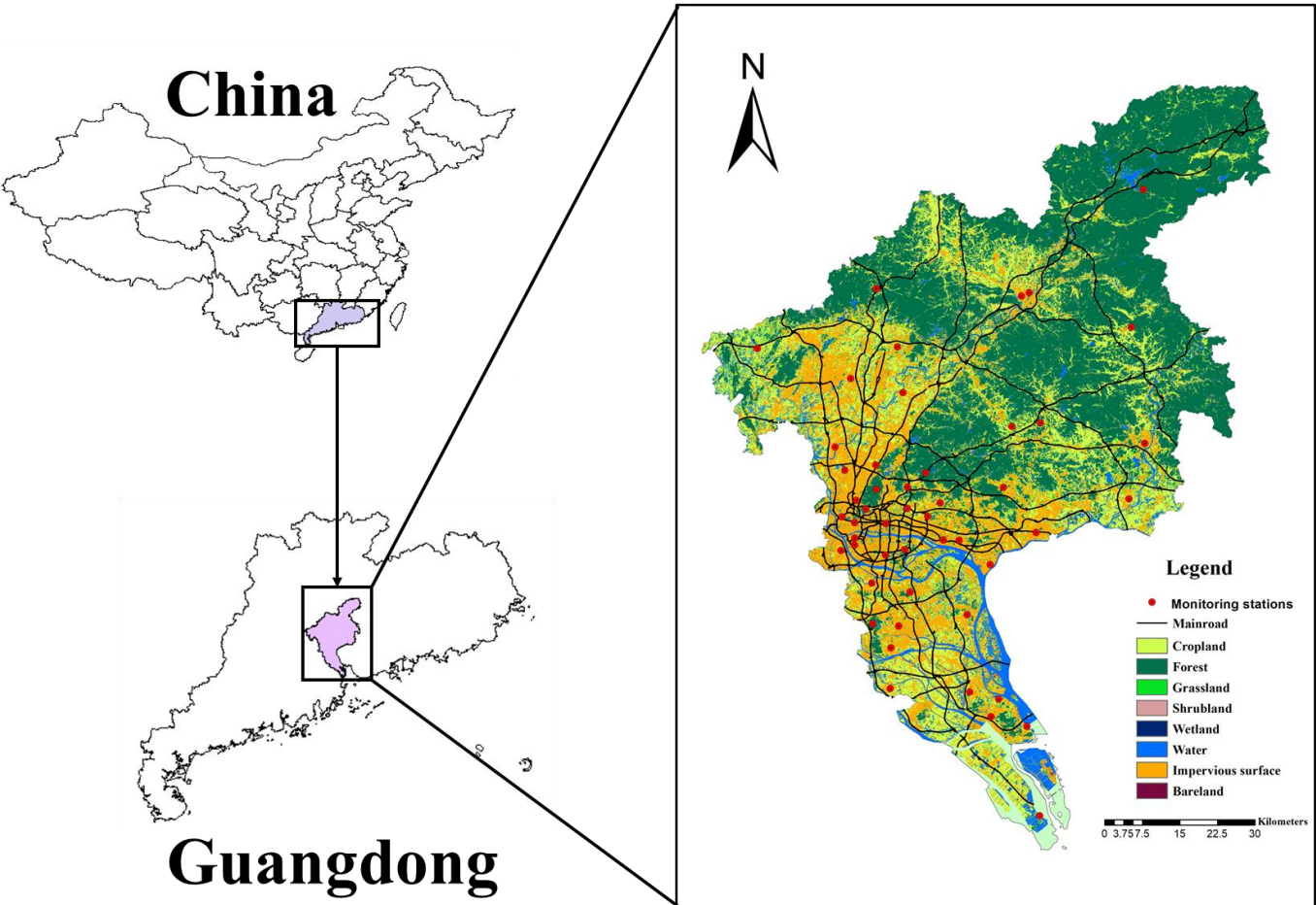
541

542

543

544 **Figure 1.** The distribution of air quality monitoring stations, land use types, and main roads  
545 in the study area.

546



547

548

549

550

551

552

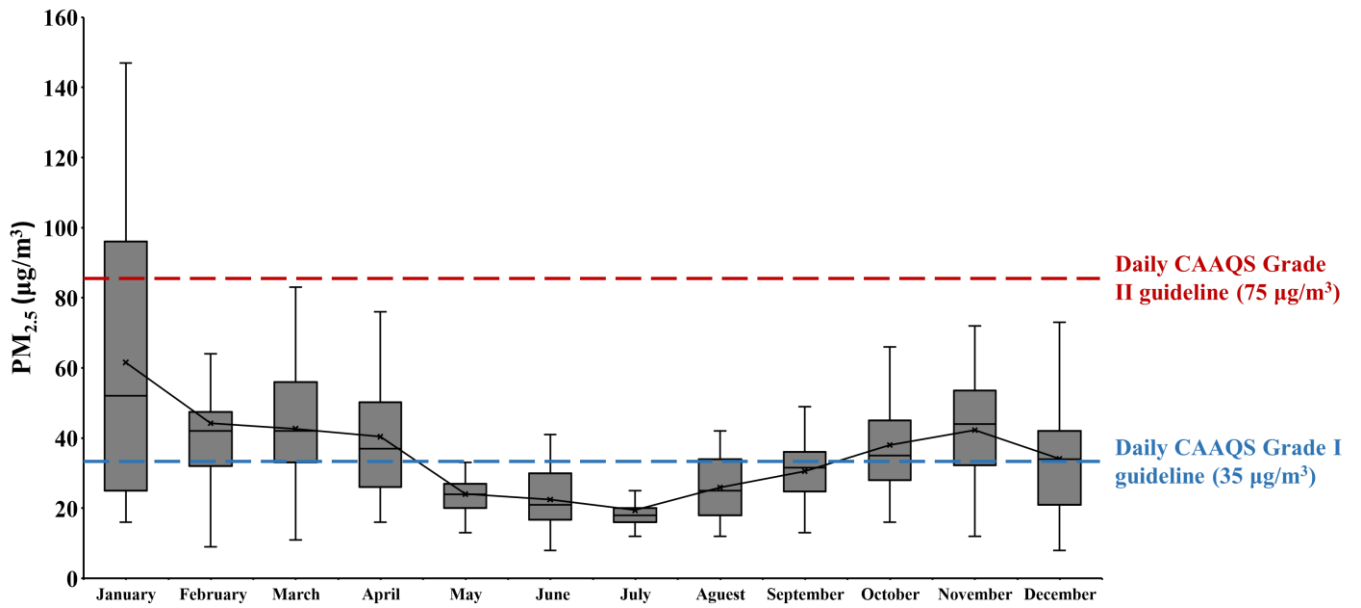
553

554

555

556 **Figure 2.** The monthly average concentrations of PM<sub>2.5</sub> in Guangzhou, China, 2018. The  
557 mean (filled circle), median (horizontal line in the box), 25<sup>th</sup> and 75<sup>th</sup> percentiles (lower  
558 and upper end of the box), 10<sup>th</sup> and 90<sup>th</sup> percentiles (lower and upper whiskers) are shown.

559



560

561

562

563

564

565

566

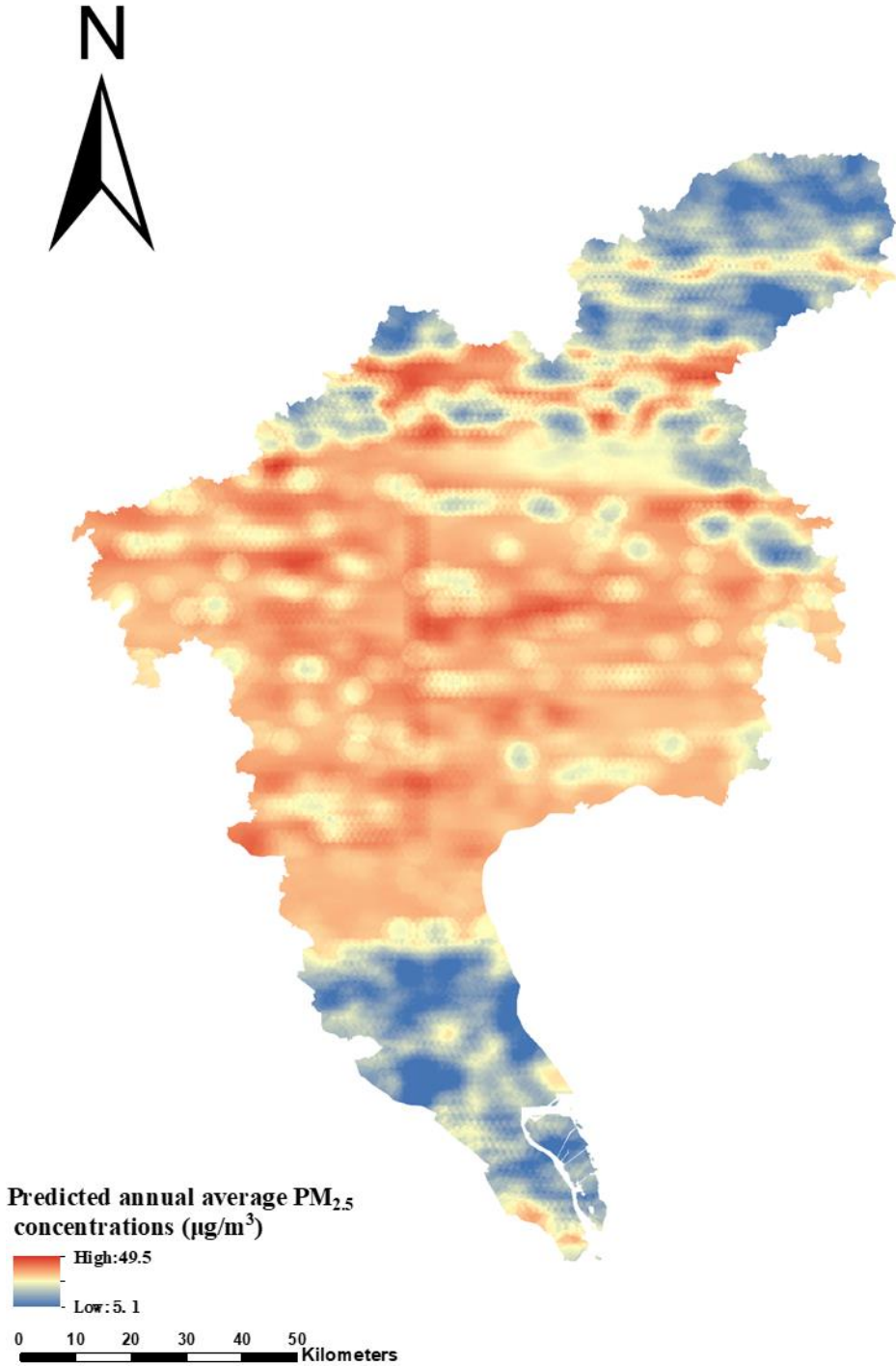
567

568

569

570

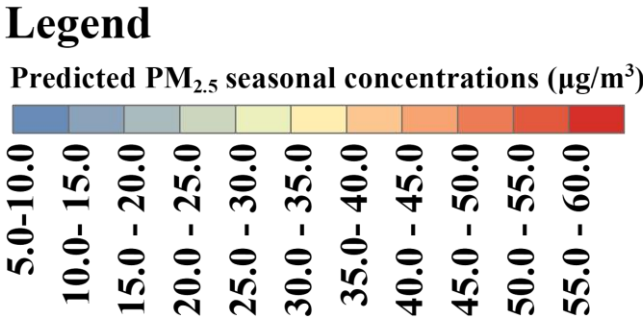
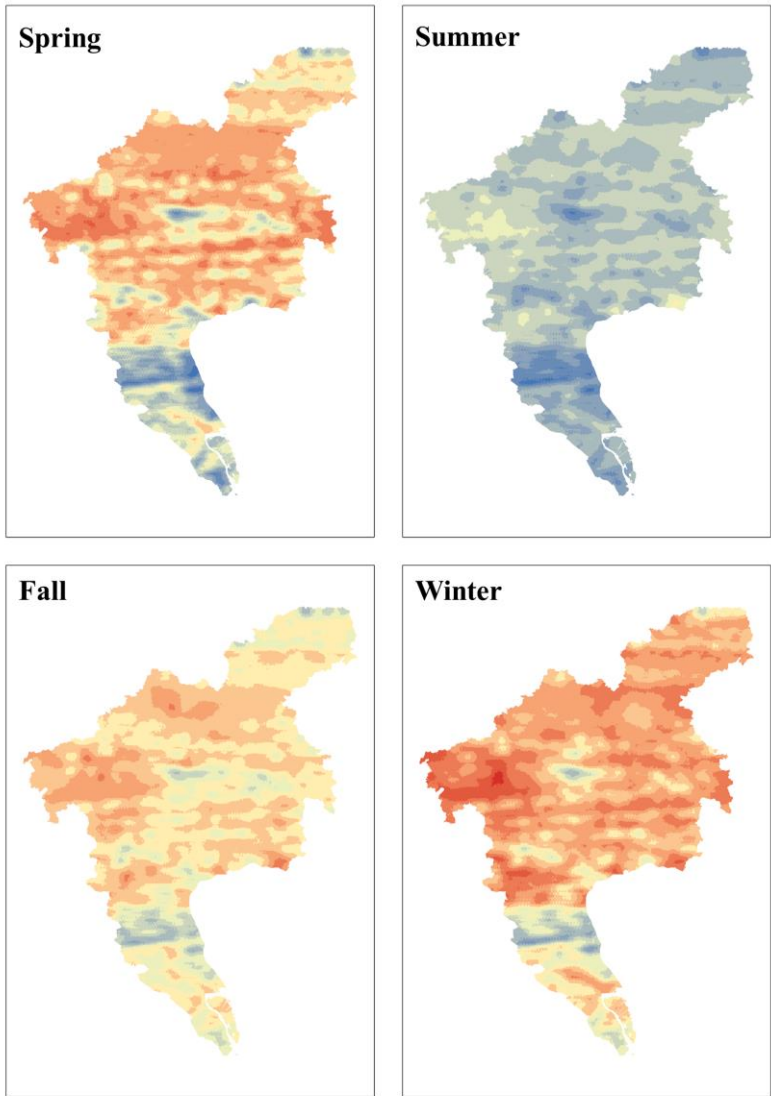
571 **Figure 3.** The spatial variation of predicted annual average PM<sub>2.5</sub> concentrations by land  
572 use regression model in Guangzhou.



573  
574  
575  
576

577 **Figure 4.** The seasonal averages of PM<sub>2.5</sub> concentrations predicted by land use regression  
578 models in Guangzhou.

579



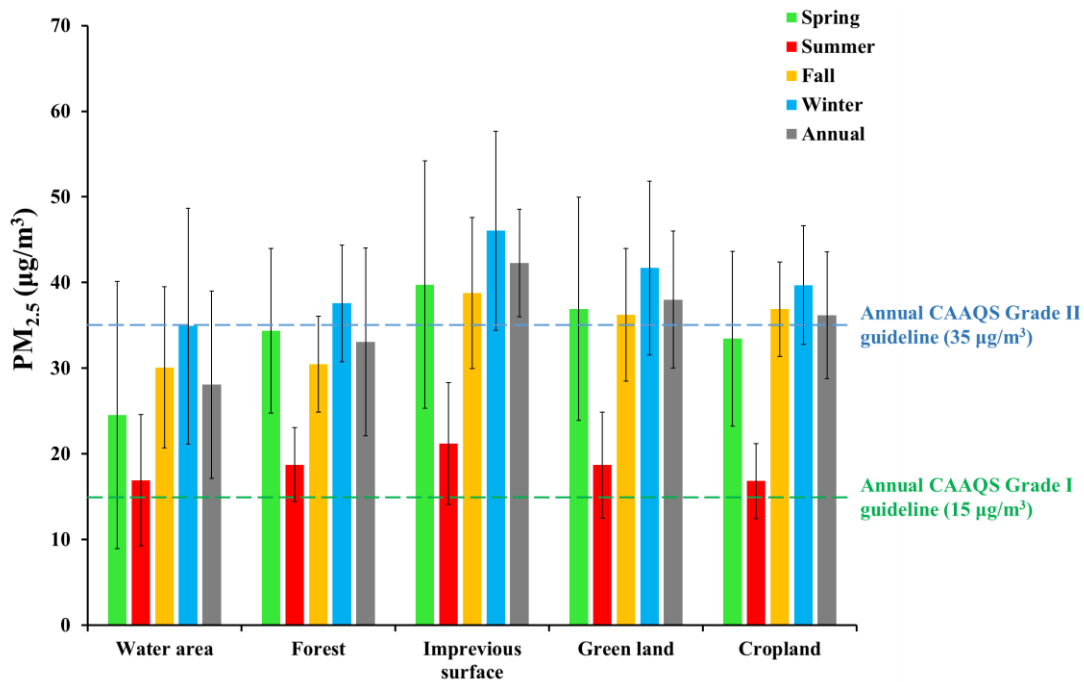
580

581

582

583

584 **Figure 5.** The seasonal and annual predicted concentrations of PM<sub>2.5</sub> in different land use  
585 types in Guangzhou. The green land is the sum of shrubland and grassland.



586

587

588

589

590

591

592

593

594

595

596

597

598 **Table1.** Potential predictor variables and expected direction of the regression coefficient  
 599 considered for the LUR model.

Categories	Predictor variables	Unit	Buffer size (radius in meters)	Assigned direction
Physical geography	DEM	m	NA	-
Socioeconomic	Population	Population/km <sup>2</sup>	NA	+
	GDP	CNY/km <sup>2</sup>	1000, 2000, 3000, 4000, 5000	+
Meteorology	Wind speed	m/s	NA	-
	Relative humidity	%	NA	NA
	Pressure	kPa	NA	NA
	Temperature	°C	NA	NA
	Boundary layer height	m	NA	-
	Precipitation	mm	NA	-
	Short wavelength radiation	W/m <sup>2</sup>	NA	NA
POI	Bus stops	Number	100, 300, 500, 700, 1000, 2000, 3000, 4000, 5000	+
			100, 300, 500, 700, 1000, 2000, 3000, 4000, 5000	+
	Parking areas	Number	100, 300, 500, 700, 1000, 2000, 3000, 4000, 5000	
Land use types	Bare land	m <sup>2</sup>	100, 300, 500, 700, 1000, 2000, 3000, 4000, 5000	+
	Cropland	m <sup>2</sup>	100, 300, 500, 700, 1000, 2000, 3000, 4000, 5000	-
	Forest	m <sup>2</sup>	100, 300, 500, 700, 1000, 2000, 3000, 4000, 5000	-
	Grassland	m <sup>2</sup>	100, 300, 500, 700, 1000, 2000, 3000, 4000, 5000	-
	Impervious surfaces	m <sup>2</sup>	100, 300, 500, 700, 1000, 2000, 3000, 4000, 5000	+
	Shrubland	m <sup>2</sup>	100, 300, 500, 700, 1000, 2000, 3000, 4000, 5000	-

	Water body	m <sup>2</sup>	100, 300, 500, 700, 1000, 2000, 3000, 4000, 5000	-
	Wetland	m <sup>2</sup>	100, 300, 500, 700, 1000, 2000, 3000, 4000, 5000	-
Impervious surfaces	Residential area	m <sup>2</sup>	100, 300, 500, 700, 1000, 2000, 3000, 4000, 5000	+
	Commercial area	m <sup>2</sup>	100, 300, 500, 700, 1000, 2000, 3000, 4000, 5000	+
	Industrial area	m <sup>2</sup>	100, 300, 500, 700, 1000, 2000, 3000, 4000, 5000	+
	Transportation area	m <sup>2</sup>	100, 300, 500, 700, 1000, 2000, 3000, 4000, 5000	+
	Public management and service area	m <sup>2</sup>	100, 300, 500, 700, 1000, 2000, 3000, 4000, 5000	+
Traffic	Length of main road	m	100, 300, 500, 700, 1000, 2000, 3000, 4000, 5000	+
	Length of highway	m	100, 300, 500, 700, 1000, 2000, 3000, 4000, 5000	+
	Length of ancillary	m	100, 300, 500, 700, 1000, 2000, 3000, 4000, 5000	+
	Length of alley	m	100, 300, 500, 700, 1000, 2000, 3000, 4000, 5000	+
Distance	Distance to nearest main road	m	NA	-
	Distance to nearest highway	m	NA	-
	Distance to nearest ancillary	m	NA	-
	Distance to nearest alley	m	NA	-
	Distance to nearest coastline	m	NA	+

**Table 2.** Annual and seasonal LUR models for PM<sub>2.5</sub> based on 49 monitoring stations in Guangzhou, China.

Predictive variables	Annual			Spring			Summer			Fall			Winter		
	$\beta^a$	<i>p</i> value	VIF <sup>b</sup>	$\beta$	<i>p</i> value	VIF									
Intercept	44.2	< 0.001	–	41.8	< 0.001	–	28.8	< 0.001	–	45.4	< 0.001	–	55.8	< 0.001	–
Length of main road (4000m)	$2.56 \times 10^{-5}$	0.001	1.50	–	–	–	–	–	–	–	–	–	–	–	–
Length of main road (3000m)	–	–	–	$6.09 \times 10^{-5}$	< 0.001	1.26	–	–	–	–	–	–	$4.50 \times 10^{-5}$	< 0.001	1.14
Length of ancillary (500 m)	–	–	–	0.001	0.01	1.3	–	–	–	–	–	–	–	–	–
DEM	-0.46	< 0.001	1.33	–	–	–	–	–	–	–	–	–	–	–	–
Distance to nearest ancillary	$-8.08 \times 10^{-3}$	< 0.001	1.04	-0.011	0.002	1.16	-0.05	0.03	1.07	$-5.66 \times 10^{-3}$	0.02	1.04	$-6.34 \times 10^{-3}$	0.03	1.05
Shrubland (5000 m)	–	–	–	–	–	–	$-9.04 \times 10^{-7}$	0.002	1.93	–	–	–	$1.84 \times 10^{-6}$	0.02	1.69
Forest (3000 m)	–	–	–	–	–	–	–	–	–	$-4.29 \times 10^{-7}$	< 0.001	1.17	–	–	–
Water (500 m)	–	–	–	$-9.13 \times 10^{-6}$	0.02	1.04	–	–	–	–	–	–	–	–	–
Commercial area (1000 m)	$4.18 \times 10^{-6}$	0.009	1.39	–	–	–	–	–	–	$6.31 \times 10^{-6}$	< 0.001	1.22	–	–	–
Commercial area (700 m)	–	–	–	–	–	–	$1.07 \times 10^{-5}$	< 0.001	1.02	–	–	–	–	–	–
Wind speed	-5.52	0.001	1.32	-5.51	0.015	1.17	-3.41	0.01	1.95	–	–	–	-6.21	0.001	1.78
Precipitation	–	–	–	–	–	–	–	–	–	-66.8	0.049	1.18	–	–	–

<sup>a</sup>  $\beta$  is the regression coefficient of each predictor variable.

<sup>b</sup> VIF is the abbreviation of Variance Inflation Factor.

**Table 3.** Comparison of performance statistics of land use regression models for PM<sub>2.5</sub>/PM<sub>10</sub> in China.

Study area	Type of monitoring data	Number of monitoring sites	PM <sub>2.5</sub> / PM <sub>10</sub>	Adjusted R <sup>2</sup>	RMSE (µg/m <sup>3</sup> )	Cross Validation R <sup>2</sup>	Cross Validation RMSE (µg/m <sup>3</sup> )	References
Annual Guangzhou				0.72	2.20	0.66	2.50	
Spring Guangzhou				0.60	2.90	0.56	2.42	
Summer Guangzhou	routine monitoring stations	49	PM <sub>2.5</sub>	0.56	1.95	0.50	2.29	This study
Fall Guangzhou				0.62	2.63	0.55	3.00	
Winter Guangzhou				0.80	2.48	0.78	2.77	
Pearl River Delta	routine monitoring stations	69	PM <sub>2.5</sub>	0.88	–	0.87	2.75	Yang et al. (2017)
Hong Kong	routine monitoring stations	15	PM <sub>2.5</sub>	0.67	–	–	2.62	Shi et al. (2017)
Hong Kong	mobile monitoring	222	PM <sub>2.5</sub>	0.63	6.52	0.61	–	Shi et al. (2016)
Hong Kong	purpose-designed monitoring	63	PM <sub>2.5</sub>	0.54	4.00	0.43	4.70	Lee et al. (2017)
Nanjing	routine monitoring stations	9	PM <sub>2.5</sub>	0.72	2.10	0.38	2.58	Huang et al. (2017)
Tianjin	routine monitoring stations	28	PM <sub>2.5</sub>	–	–	0.73	6.38	Chen et al. (2017c)
Shanghai	routine monitoring stations	35	PM <sub>2.5</sub>	0.88	–	–	–	Liu et al. (2016)
Beijing	routine monitoring stations	35	PM <sub>2.5</sub>	0.68	–	–	–	Hu et al. (2016)
Beijing	routine monitoring stations	35	PM <sub>2.5</sub>	0.58	–	–	9.30	Wu et al. (2015)
Lanzhou	purpose-designed monitoring	38	PM <sub>2.5</sub>	0.73	9.60	0.67	–	Jin et al. (2019)
Yantai	purpose-designed monitoring	29	PM <sub>2.5</sub>	0.65	3.12	0.56	–	Cai et al. (2020)
Changsha	routine monitoring stations and purpose-designed monitoring	36	PM <sub>10</sub>	0.62	9.00	0.58	–	Liu et al. (2015)
Changsha	purpose-designed monitoring	40	PM <sub>10</sub>	0.51	5.60	0.60	–	Li et al. (2015)

Tianjin	routine monitoring stations	30	PM <sub>10</sub>	0.84	0.21	–	–	Shang et al. (2012)
Wuhan	routine monitoring stations	9	PM <sub>10</sub>	0.59	–	–	–	Xu et al. (2016)
Shanghai	routine monitoring stations	28	PM <sub>10</sub>	0.80	4.20	0.73	5.00	Meng et al. (2016)

---

**Table 4.** Estimated avoided premature mortality and benefits of health effects associated with PM<sub>2.5</sub> reduction in Guangzhou.

Health endpoints	Avoided cases (person)		Benefits (Million CNY)	
	Mean	95% CI	Mean	95% CI
All cause	992	221–2140	1478	257–2425
Cardiovascular	362	124–768	567	48–924
Respiratory	92	-18–176	139	24–278

## References:

- Anand JS, Monks PS. Estimating daily surface NO<sub>2</sub> concentrations from satellite data—a case study over Hong Kong using land use regression models. *Atmospheric Chemistry & Physics* 2017; 17.
- Beelen R, Hoek G, Vienneau D, Eeftens M, Dimakopoulou K, et al. Development of NO<sub>2</sub> and NO<sub>x</sub> land use regression models for estimating air pollution exposure in 36 study areas in Europe - The ESCAPE project. *Atmospheric Environment* 2013; 72: 10-23.
- Beelen R, Raaschou-Nielsen O, Stafoggia M, Andersen ZJ, Weinmayr G, Hoffmann B, et al. Effects of long-term exposure to air pollution on natural-cause mortality: an analysis of 22 European cohorts within the multicentre ESCAPE project. *The Lancet* 2014; 383: 785-795.
- Briggs DJ, Collins S, Elliott P, Fischer P, Kingham S, Lebreton E, et al. Mapping urban air pollution using GIS: a regression-based approach. *International Journal of Geographical Information Science* 1997; 11: 699-718.
- Cai J, Ge Y, Li H, Yang C, Liu C, Meng X, et al. Application of land use regression to assess exposure and identify potential sources in PM<sub>2.5</sub>, BC, NO<sub>2</sub> concentrations. *Atmospheric Environment* 2020; 223: 117267.
- Chen G, Li S, Knibbs LD, Hamm NA, Cao W, Li T, et al. A machine learning method to estimate PM<sub>2.5</sub> concentrations across China with remote sensing, meteorological and land use information. *Science of the Total Environment* 2018a; 636: 52-60.
- Chen L, Gao S, Zhang H, Sun Y, Ma Z, Vedal S, et al. Spatiotemporal modeling of PM<sub>2.5</sub> concentrations at the national scale combining land use regression and Bayesian maximum entropy in China. *Environment international* 2018b; 116: 300-307.
- Chen L, Liu C, Zhang L, Zou R, Zhang Z. Variation in tree species ability to capture and retain airborne fine particulate matter (PM<sub>2.5</sub>). *Scientific reports* 2017a; 7: 1-11.
- Chen L, Shi M, Gao S, Li S, Mao J, Zhang H, et al. Assessment of population exposure to PM<sub>2.5</sub> for mortality in China and its public health benefit based on BenMAP. *Environmental Pollution* 2017b; 221: 311-317.
- Chen L, Shi M, Li S, Bai Z, Wang Z. Combined use of land use regression and BenMAP for estimating public health benefits of reducing PM<sub>2.5</sub> in Tianjin, China. *Atmospheric Environment* 2017c; 152: 16-23.
- Chen R, Kan H, Chen B, Huang W, Bai Z, Song G, et al. Association of particulate air pollution with daily mortality: the China Air Pollution and Health Effects Study. *American journal of epidemiology* 2012; 175: 1173-1181.
- Chen Z, Xie X, Cai J, Chen D, Gao B, He B, et al. Understanding meteorological influences on PM<sub>2.5</sub>

- concentrations across China: a temporal and spatial perspective. *Atmospheric Chemistry and Physics* 2018c; 18: 5343.
- Davidson K, Hallberg A, McCubbin D, Hubbell B. Analysis of PM<sub>2.5</sub> using the environmental benefits mapping and analysis program (BenMAP). *Journal of Toxicology and Environmental Health, Part A* 2007; 70: 332-346.
- de Hoogh K, Gulliver J, van Donkelaar A, Martin RV, Marshall JD, Bechle MJ, et al. Development of West-European PM<sub>2.5</sub> and NO<sub>2</sub> land use regression models incorporating satellite-derived and chemical transport modelling data. *Environmental research* 2016; 151: 1-10.
- de Hoogh K, Korek M, Vienneau D, Keuken M, Kukkonen J, Nieuwenhuijsen MJ, et al. Comparing land use regression and dispersion modelling to assess residential exposure to ambient air pollution for epidemiological studies. *Environment international* 2014; 73: 382-392.
- DeMocker MJ. *Benefits and Costs of the Clean Air Act 1990-2020: Revised Analytical Plan For EPA's Second Prospective Analysis*. Industrial Economics Incorporated, Cambridge, MA 2003.
- Eeftens M, Beelen R, de Hoogh K, Bellander T, Cesaroni G, Cirach M, et al. Development of land use regression models for PM<sub>2.5</sub>, PM<sub>2.5</sub> absorbance, PM<sub>10</sub> and PM<sub>coarse</sub> in 20 European study areas; results of the ESCAPE project. *Environmental science & technology* 2012a; 46: 11195-11205.
- Eeftens M, Beelen R, Hoogh KD, Bellander T, Hoek G. Development of Land Use Regression models for PM(2.5), PM(2.5) absorbance, PM(10) and PM(coarse) in 20 European study areas; results of the ESCAPE project. *Environmental Science & Technology* 2012b; 46: 11195-11205.
- Eeftens M, Tsai MY, Ampe C, Anwander B, Beelen R, Bellander T, et al. Variation of PM<sub>2.5</sub>, PM<sub>10</sub>, PM<sub>2.5</sub> absorbance and PM coarse concentrations between and within 20 European study areas - results of the ESCAPE project. *Atmospheric Environment* 2012c; 62: 303-317.
- He B, Heal MR, ID, Reis S. Land-Use Regression Modelling of Intra-Urban Air Pollution Variation in China: Current Status and Future Needs. *Atmosphere* 2018; 9.
- Henderson SB, Beckerman B, Jerrett M, Brauer M. Application of Land Use Regression to Estimate Long-Term Concentrations of Traffic-Related Nitrogen Oxides and Fine Particulate Matter. *Environmental ence & Technology* 2007; 41: 2422-8.
- Hoek G, Beelen R, De Hoogh K, Vienneau D, Gulliver J, Fischer P, et al. A review of land-use regression models to assess spatial variation of outdoor air pollution. *Atmospheric environment* 2008; 42: 7561-7578.
- Hsieh M-T, Peng C-Y, Chung W-Y, Lai C-H, Huang S-K, Lee C-L. Simulating the spatiotemporal distribution of BTEX with an hourly grid-scale model. *Chemosphere* 2020; 246: 125722.
- Hu L, Liu J, He Z. Self-adaptive revised land use regression models for estimating PM<sub>2.5</sub> concentrations in Beijing, China. *Sustainability* 2016; 8: 786.

- Huang L, Zhang C, Bi J. Development of land use regression models for PM<sub>2.5</sub>, SO<sub>2</sub>, NO<sub>2</sub> and O<sub>3</sub> in Nanjing, China. *Environmental research* 2017; 158: 542-552.
- Huang R-J, Zhang Y, Bozzetti C, Ho K-F, Cao J-J, Han Y, et al. High secondary aerosol contribution to particulate pollution during haze events in China. *Nature* 2014; 514: 218-222.
- Jin L, Berman JD, Warren JL, Levy JI, Thurston G, Zhang Y, et al. A land use regression model of nitrogen dioxide and fine particulate matter in a complex urban core in Lanzhou, China. *Environmental research* 2019; 177: 108597.
- Jones AM, Harrison RM. Estimation of the emission factors of particle number and mass fractions from traffic at a site where mean vehicle speeds vary over short distances. *Atmospheric Environment* 2006; 40: 7125-7137.
- Kheirbek I, Haney J, Douglas S, Ito K, Caputo Jr S, Matte T. The public health benefits of reducing fine particulate matter through conversion to cleaner heating fuels in New York City. *Environmental science & technology* 2014; 48: 13573-13582.
- Lai S, Zhao Y, Ding A, Zhang Y, Song T, Zheng J, et al. Characterization of PM<sub>2.5</sub> and the major chemical components during a 1-year campaign in rural Guangzhou, Southern China. *Atmospheric Research* 2016; 167: 208-215.
- Lee C-L, Huang H-C, Wang C-C, Sheu C-C, Wu C-C, Leung S-Y, et al. A new grid-scale model simulating the spatiotemporal distribution of PM<sub>2.5</sub>-PAHs for exposure assessment. *Journal of hazardous materials* 2016; 314: 286-294.
- Lee H, Liu Y, Coull B, Schwartz J, Koutrakis P. A novel calibration approach of MODIS AOD data to predict PM 2.5 concentrations. *Atmospheric Chemistry & Physics Discussions* 2011; 11.
- Lee M, Brauer M, Wong P, Tang R, Tsui TH, Choi C, et al. Land use regression modelling of air pollution in high density high rise cities: A case study in Hong Kong. *Science of the Total Environment* 2017; 592: 306-315.
- Li J, Zhu Y, Kelly JT, Jang CJ, Wang S, Hanna A, et al. Health benefit assessment of PM<sub>2.5</sub> reduction in Pearl River Delta region of China using a model-monitor data fusion approach. *Journal of environmental management* 2019; 233: 489-498.
- Li X, Liu W, Chen Z, Zeng G, Hu C, León T, et al. The application of semicircular-buffer-based land use regression models incorporating wind direction in predicting quarterly NO<sub>2</sub> and PM<sub>10</sub> concentrations. *Atmospheric Environment* 2015; 103: 18-24.
- Lim JM, Jeong JH, Lee JH, Moon JH, Chung YS, Kim KH. The analysis of PM<sub>2.5</sub> and associated elements and their indoor/outdoor pollution status in an urban area. *Indoor Air* 2011; 21: 145-155.
- Liu C, Henderson BH, Wang D, Yang X, Peng Z-r. A land use regression application into assessing spatial variation of intra-urban fine particulate matter (PM<sub>2.5</sub>) and nitrogen dioxide (NO<sub>2</sub>) concentrations in City of Shanghai, China. *Science of The Total Environment* 2016; 565: 607-615.

- Liu J, Li J, Zhang Y, Liu D, Ding P, Shen C, et al. Source apportionment using radiocarbon and organic tracers for PM<sub>2.5</sub> carbonaceous aerosols in Guangzhou, South China: Contrasting local-and regional-scale haze events. *Environmental science & technology* 2014; 48: 12002-12011.
- Liu W, Li X, Chen Z, Zeng G, León T, Liang J, et al. Land use regression models coupled with meteorology to model spatial and temporal variability of NO<sub>2</sub> and PM<sub>10</sub> in Changsha, China. *Atmospheric environment* 2015; 116: 272-280.
- Luo G, Zhang L, Hu X, Qiu R. Quantifying public health benefits of PM<sub>2.5</sub> reduction and spatial distribution analysis in China. *Science of The Total Environment* 2020; 719: 137445.
- Ma Z, Hu X, Sayer AM, Levy R, Zhang Q, Xue Y, et al. Satellite-based spatiotemporal trends in PM<sub>2.5</sub> concentrations: China, 2004–2013. *Environmental health perspectives* 2016; 124: 184-192.
- Meng X, Chen L, Cai J, Zou B, Wu C-F, Fu Q, et al. A land use regression model for estimating the NO<sub>2</sub> concentration in Shanghai, China. *Environmental research* 2015; 137: 308-315.
- Meng X, Fu Q, Ma Z, Chen L, Zou B, Zhang Y, et al. Estimating ground-level PM<sub>10</sub> in a Chinese city by combining satellite data, meteorological information and a land use regression model. *Environmental Pollution* 2016; 208: 177-184.
- Nguyen T, Yu X, Zhang Z, Liu M, Liu X. Relationship between types of urban forest and PM<sub>2.5</sub> capture at three growth stages of leaves. *Journal of Environmental Sciences* 2015; 27: 33-41.
- Nowak DJ, Hirabayashi S, Doyle M, McGovern M, Pasher J. Air pollution removal by urban forests in Canada and its effect on air quality and human health. *Urban Forestry & Urban Greening* 2018; 29: 40-48.
- Pan X, Li G, Gao T. Hazardous breathing: Health hazards and economic loss assessment studies for PM<sub>2.5</sub>. <https://finance.huanqiu.com/article/9CaKrnJyfs6> 2012.
- Robinson LA. Valuing the health impacts of air emissions. 2011.
- Rosenlund M, Forastiere F, Stafoggia M, Porta D, Perucci M, Ranzi A, et al. Comparison of regression models with land-use and emissions data to predict the spatial distribution of traffic-related air pollution in Rome. *Journal of Exposure Science & Environmental Epidemiology* 2007; 18: 192-199.
- Sabaliauskas K, Jeong CH, Yao X, Reali C, Sun T, Evans GJ. Development of a land-use regression model for ultrafine particles in Toronto, Canada. *Atmospheric Environment* 2015; 110: 84-92.
- Sacks JD, Lloyd JM, Zhu Y, Anderton J, Jang CJ, Hubbell B, et al. The Environmental Benefits Mapping and Analysis Program–Community Edition (BenMAP–CE): A tool to estimate the health and economic benefits of reducing air pollution. *Environmental Modelling & Software* 2018; 104: 118-129.
- Sampson PD, Richards M, Szpiro AA, Bergen S, Sheppard L, Larson TV, et al. A regionalized national universal kriging model using Partial Least Squares regression for estimating annual PM<sub>2.5</sub>

- concentrations in epidemiology. *Atmospheric environment* 2013; 75: 383-392.
- Selmi W, Weber C, Rivière E, Blond N, Mehdi L, Nowak D. Air pollution removal by trees in public green spaces in Strasbourg city, France. *Urban Forestry & Urban Greening* 2016; 17: 192-201.
- Shang Y, Chen C, Li Y, Zhao J, Zhu T. Hydroxyl radical generation mechanism during the redox cycling process of 1,4-naphthoquinone. *Environmental Science & Technology* 2012; 46: 2935.
- Shen F, Zhang L, Jiang L, Tang M, Gai X, Chen M, et al. Temporal variations of six ambient criteria air pollutants from 2015 to 2018, their spatial distributions, health risks and relationships with socioeconomic factors during 2018 in China. *Environment International* 2020; 137: 105556.
- Shi Y, Lau KK-L, Ng E. Developing street-level PM<sub>2.5</sub> and PM<sub>10</sub> land use regression models in high-density Hong Kong with urban morphological factors. *Environmental science & technology* 2016; 50: 8178-8187.
- Shi Y, Lau KK-L, Ng E. Incorporating wind availability into land use regression modelling of air quality in mountainous high-density urban environment. *Environmental research* 2017; 157: 17-29.
- Solomos S, Amiridis V, Zanis P, Gerasopoulos E, Sofiou F, Herekakis T, et al. Smoke dispersion modeling over complex terrain using high resolution meteorological data and satellite observations—The FireHub platform. *Atmospheric Environment* 2015; 119: 348-361.
- Stafoggia M, Cesaroni G, Peters A, Andersen ZJ, Badaloni C, Beelen R, et al. Long-term exposure to ambient air pollution and incidence of cerebrovascular events: results from 11 European cohorts within the ESCAPE project. *Environmental health perspectives* 2014; 122: 919-925.
- Tang R, Tian L, Thach T-Q, Tsui TH, Brauer M, Lee M, et al. Integrating travel behavior with land use regression to estimate dynamic air pollution exposure in Hong Kong. *Environment international* 2018; 113: 100-108.
- Vienneau D, De Hoogh K, Bechle MJ, Beelen R, Van Donkelaar A, Martin RV, et al. Western European land use regression incorporating satellite-and ground-based measurements of NO<sub>2</sub> and PM<sub>10</sub>. *Environmental science & technology* 2013; 47: 13555-13564.
- Voorhees AS, Wang J, Wang C, Zhao B, Wang S, Kan H. Public health benefits of reducing air pollution in Shanghai: a proof-of-concept methodology with application to BenMAP. *Science of the total environment* 2014; 485: 396-405.
- Vos PEJ, Maiheu B, Vankerkom J, Janssen S. Improving local air quality in cities: To tree or not to tree? *Environmental Pollution* 2013; 183: 113-122.
- Wang H, Maher BA, Ahmed IA, Davison B. Efficient removal of ultrafine particles from diesel exhaust by selected tree species: implications for roadside planting for improving the quality of urban air. *Environmental science & technology* 2019; 53: 6906-6916.
- Wang N, Ling Z, Deng X, Deng T, Lyu X, Li T, et al. Source contributions to PM<sub>2.5</sub> under unfavorable weather conditions in Guangzhou City, China. *Advances in Atmospheric Sciences* 2018; 35: 1145-

- Wang X, Yin H, Ge Y, Yu L, Xu Z, Yu C, et al. On-vehicle emission measurement of a light-duty diesel van at various speeds at high altitude. *Atmospheric Environment* 2013; 81: 263-269.
- West JJ, Cohen A, Dentener F, Brunekreef B, Zhu T, Armstrong B, et al. What we breathe impacts our health: improving understanding of the link between air pollution and health. ACS Publications, 2016.
- Wu D, Tie X, Li C, Ying Z, Lau AK-H, Huang J, et al. An extremely low visibility event over the Guangzhou region: A case study. *Atmospheric Environment* 2005; 39: 6568-6577.
- Wu J, Li J, Peng J, Li W, Xu G, Dong C. Applying land use regression model to estimate spatial variation of PM 2.5 in Beijing, China. *Environmental Science and Pollution Research* 2015; 22: 7045-7061.
- Wu Y, Wang W, Liu C, Chen R, Kan H. The association between long-term fine particulate air pollution and life expectancy in China, 2013 to 2017. *Science of The Total Environment* 2020: 136507.
- Xu G, Jiao L, Zhao S, Yuan M, Li X, Han Y, et al. Examining the impacts of land use on air quality from a spatio-temporal perspective in Wuhan, China. *Atmosphere* 2016; 7: 62.
- Yang X, Zheng Y, Geng G, Liu H, Man H, Lv Z, et al. Development of PM<sub>2.5</sub> and NO<sub>2</sub> models in a LUR framework incorporating satellite remote sensing and air quality model data in Pearl River Delta region, China. *Environmental pollution* 2017; 226: 143-153.
- Young MT, Bechle MJ, Sampson PD, Szpiro AA, Marshall JD, Sheppard L, et al. Satellite-based NO<sub>2</sub> and model validation in a national prediction model based on universal kriging and land-use regression. *Environmental science & technology* 2016; 50: 3686-3694.
- Yuan C, Ng E, Norford LK. Improving air quality in high-density cities by understanding the relationship between air pollutant dispersion and urban morphologies. *Building and Environment* 2014; 71: 245-258.
- Yuan Q, Lai S, Song J, Ding X, Zheng L, Wang X, et al. Seasonal cycles of secondary organic aerosol tracers in rural Guangzhou, Southern China: The importance of atmospheric oxidants. *Environmental Pollution* 2018; 240: 884-893.
- Zang Z, Wang W, You W, Li Y, Ye F, Wang C. Estimating ground-level PM<sub>2.5</sub> concentrations in Beijing, China using aerosol optical depth and parameters of the temperature inversion layer. *Science of the Total Environment* 2017; 575: 1219-1227.
- Zhang JJY, Sun L, Barrett O, Bertazzon S, Underwood FE, Johnson M. Development of land-use regression models for metals associated with airborne particulate matter in a North American city. *Atmospheric Environment* 2015a; 106: 165-177.
- Zhang X, Chen B, Fan X. Different fuel types and heating approaches impact on the indoor air quality of rural houses in Northern China. *Procedia Engineering* 2015b; 121: 493-500.
- Zhang Y, Bocquet M, Mallet V, Seigneur C, Baklanov A. Real-time air quality forecasting, part I: History,